Cerebral Cortex
Supplemental Information

Differential Recruitment of Dentate Gyrus Interneuron Types by Commissural versus Perforant Pathways

Tsan-Ting Hsu, Cheng-Ta Lee, Ming-Hong Tai, Cheng-Chang Lien

Supplemental Information

Supplemental Figures

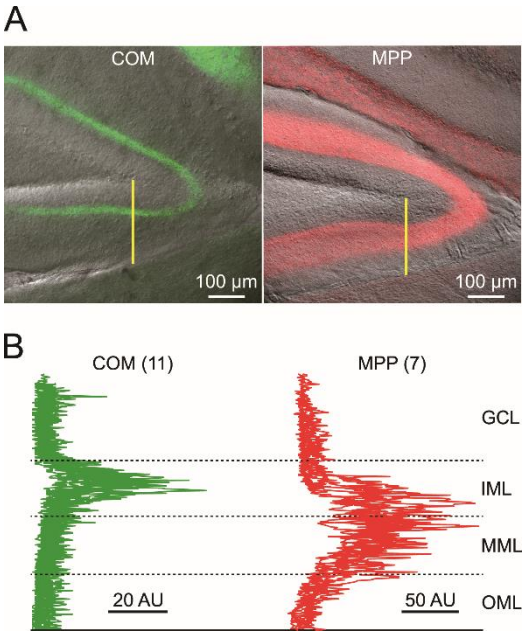

Figure S1. ChR2 expression in the COM or MPP

(*A*) Analysis of ChR2-eYFP in the COM (green) or ChR2-mCherry (red) in the MPP in fixed slices. A straight, one-pixel wide yellow line drawn from the crest of GCL/hilus border to the edge of lower blade of molecular layer defined the region of interest (ROI) in which the fluorescent intensity was quantified. (*B*) The fluorescence intensity was plotted against the normalized distance across different layers of the DG. Green and red traces: intensity profiles of selected ROIs. Numbers of analyzed slices are given in parentheses. AU: arbitrary unit, intensity value ranging from min-max is 0 to 255 in 8-bit image.

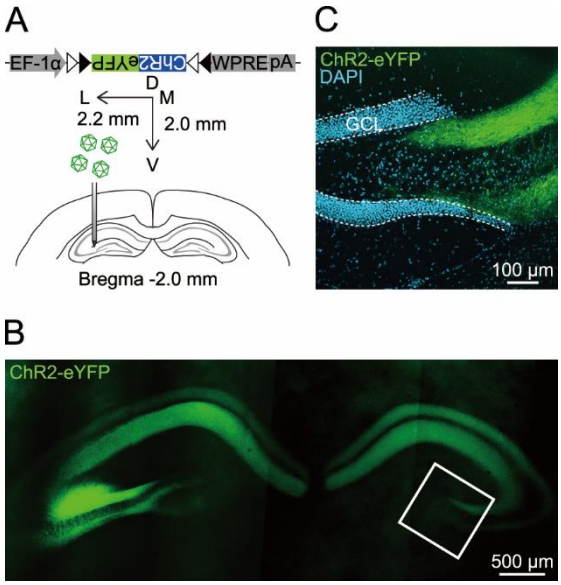

Figure S2. Selective ChR2 expression in CA3 neurons

(*A*) Schematic diagram illustrates unilateral injection of a viral vector AAV5-EF1α-DIO-ChR2-eYFP into the CA3 region of the dorsal hippocampus. (*B*) Fluorescence image of ChR2-eYFP expression in the dorsal hippocampus. The injection site is restricted in the CA3 region of the left dorsal hippocampus. The boxed area is shown at a higher magnification in (*C*) ChR2-eYFP expression (green) in the strata radiatum and oriens of the CA3 region and GCs are labeled with DAPI. The borders of the GCL are outlined. Note the lack of ChR2-eYFP expression in the IML of the contralateral DG.

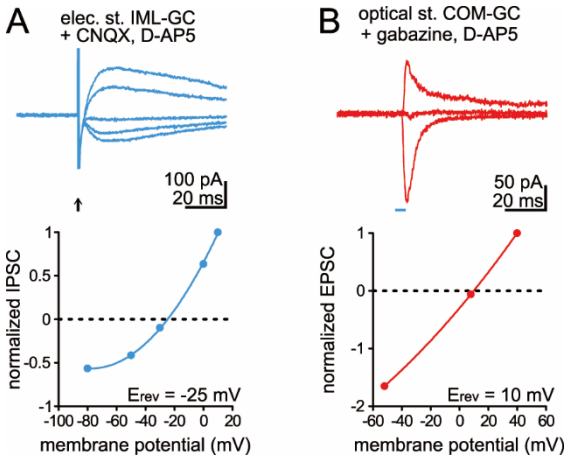

Figure S3. Reversal potentials of EPSCs and IPSCs

(*A*) Electrically evoked IPSCs recorded in the presence of the AMPA receptor antagonist CNQX (10 μM) and NMDA receptor antagonist D-AP5 (50 μM) had a reversal potential near –25 mV. (*B*) Optically evoked EPSCs recorded in the presence of the $GABA_A$ receptor antagonist gabazine (1 μM) and NMDA receptor antagonist D-AP5 (50 μM) had a reversal potential near 10 mV. Data points were fitted with second order polynomials.

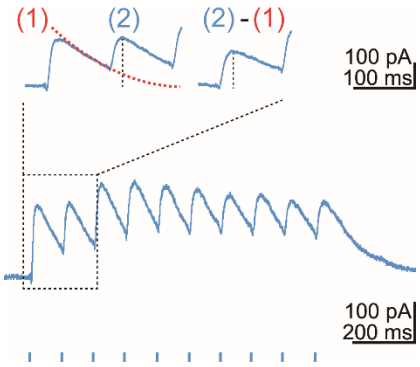

Figure S4. Calculation of IPSC amplitudes during repeated photo-stimulation

The peak amplitude of each IPSC was calibrated by subtracting the decay (red dotted line) of previous IPSC. The red dotted line is the mono-exponential fit of the IPSC decay.

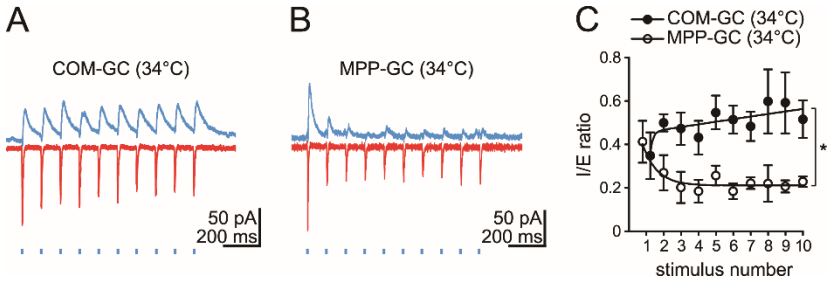

Figure S5. Distinct I/E ratios at COM-GC and MPP-GC synapses during repetitive stimulation at physiological temperature

(*A*, *B*) Traces: EPSCs (red, V_{hold} = –30 mV) and IPSCs (blue, V_{hold} = 12 mV) evoked by 10 Hz photo-stimulation of COM (*A*) or MPP (*B*) at 34℃. The blue bar indicates the light pulse. (*C*) Summary of the I/E ratio versus stimulus number during 10 Hz photo-stimulation of COM (*n* = 4) or MPP (*n* = 4) at 34℃. **P* < 0.05. Data are expressed as mean ± SEM.

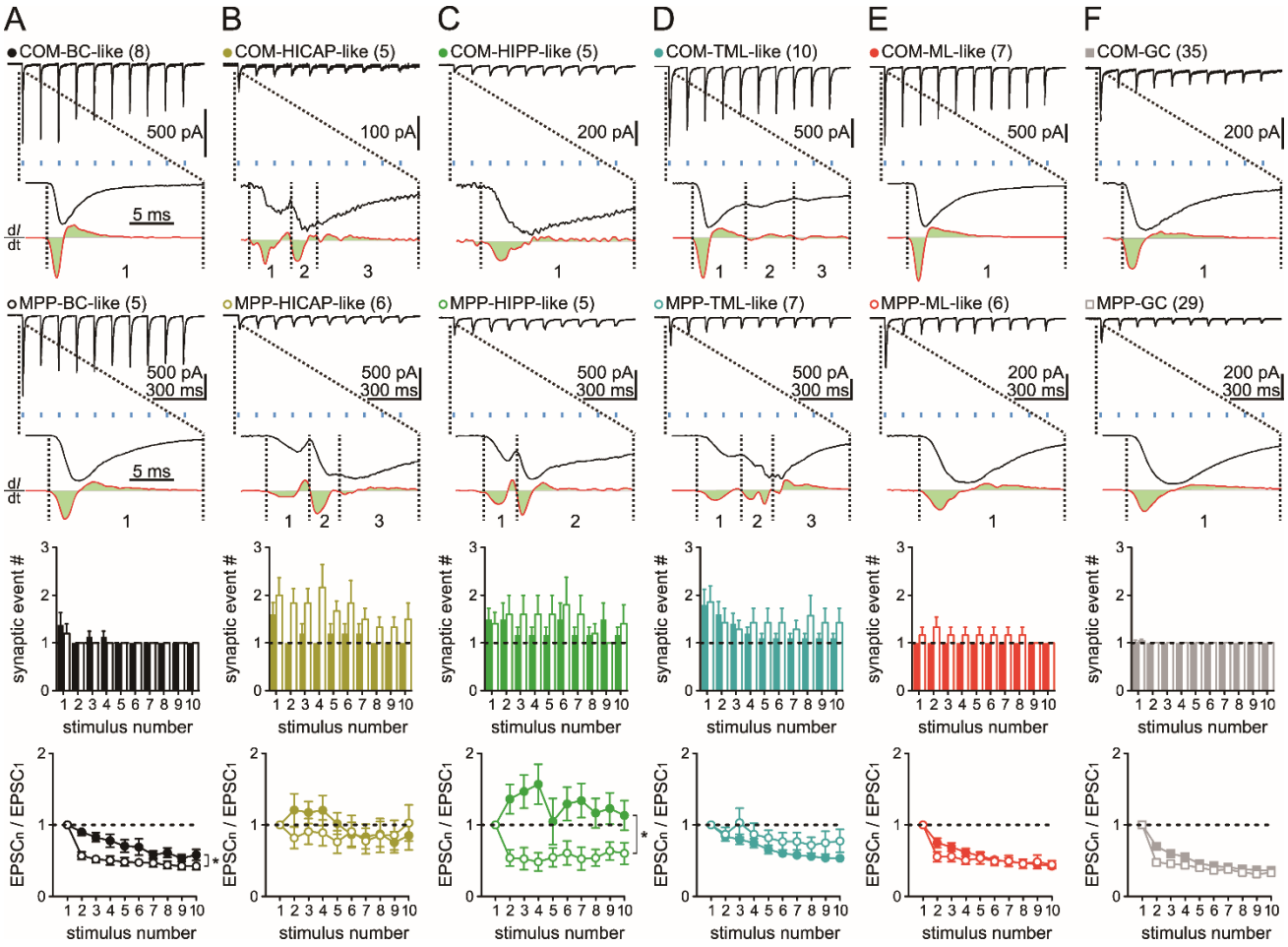

Figure S6. Synaptic events during photo-stimulation of COM or MPP

(*A–F*) EPSCs evoked by 10 Hz photo-stimulation (blue) of COM and MPP in various IN subtypes and GCs. The EPSC traces following the first light pulse and their corresponding first derivatives (red traces) were shown at higher magnification. Synaptic events were indicated by numbers. Middle and bottom, summary plots of light-evoked EPSC event number and short-term dynamics in EPSCs across 10 Hz trains (normalized to $EPSC_1$) versus stimulus number. Notice that the short-term dynamics of COM-BC-like IN synapses is significantly different from that of MPP-BC-like IN synapses. Moreover,

COM-HIPP-like IN synapses are facilitating, in great contrast to depression of MPP-HIPP-like IN synapses. *$P < 0.05$. Numbers of cells are given in parentheses. Data are expressed as mean ± SEM.

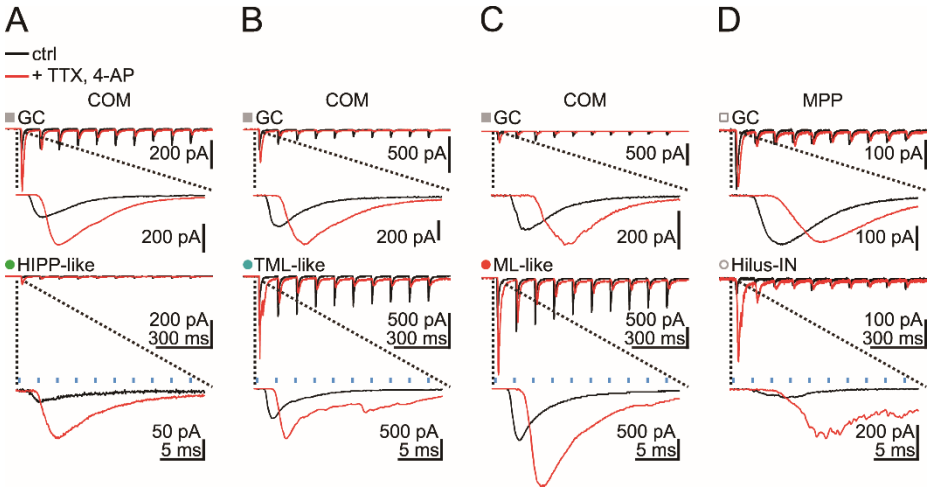

Figure S7. Comparison of light-evoked EPSCs in GC and IN synapses before and after isolating monosynaptic responses by Na^+ and K^+ channel blockers

(*A–D*) EPSCs evoked by 10 Hz photo-stimulation (blue) of COM and MPP in GCs (top) and simultaneously recorded INs (bottom) before (ctrl, black traces) and after TTX (1 μM) and 4-AP (1 mM) application (+TTX, 4-AP, red traces). The EPSC traces following the first light pulse were shown at higher magnification. Notice that the synaptic delays of EPSCs were shorter than those measured in the presence of TTX and 4-AP.

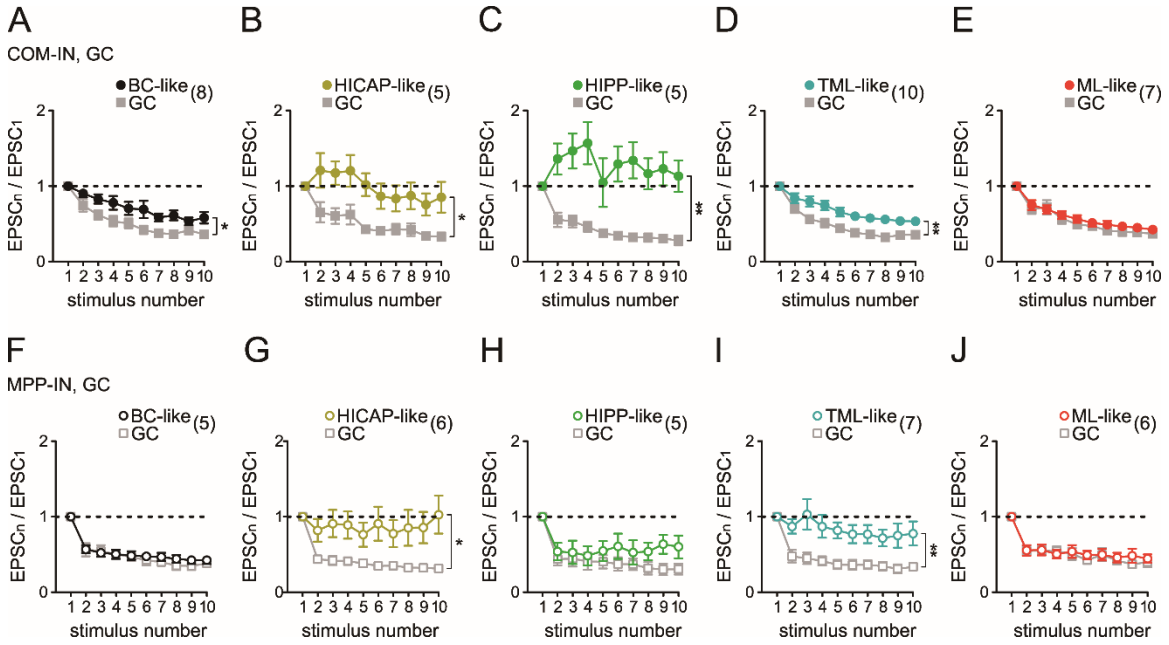

Figure S8. Comparison of short-term dynamics of EPSCs between INs and simultaneously recorded GCs evoked by COM and MPP 10 Hz train photo-stimulation

(*A–E*) Summary plots of short-term dynamics of EPSCs in individual IN subtypes and simultaneously recorded GCs across 10 Hz train photo-stimulation of COM (normalized to $EPSC_1$) versus stimulus number. (*F–J*) Summary plots of short-term dynamics of EPSCs in each IN subtype and the simultaneously recorded GCs across 10 Hz train photo-stimulation of MPP (normalized to $EPSC_1$) versus stimulus number. $*P < 0.05$; $**P < 0.01$. Numbers of dual-recording pairs are given in parentheses. Data are expressed as mean ± SEM.

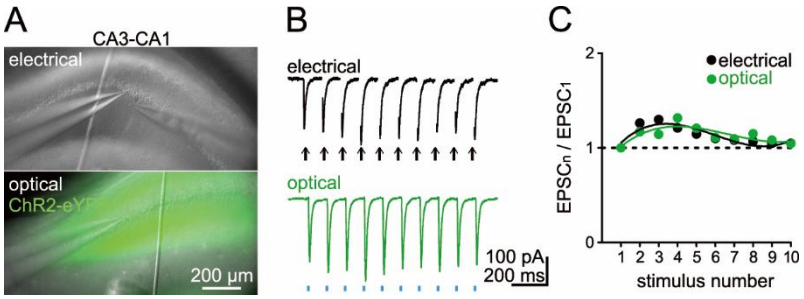

Figure S9. Comparison of AAV5-ChR2 activation and electrical stimulation at CA3–CA1 synapses

(*A*) Upper, electrical stimulation of Schaffer collateral axons and recording of EPSCs from a CA1 pyramidal cell. Left pipette, recording electrode; right pipette, stimulation electrode. Lower, ChR2 expression in Schaffer collateral axons and recording of optically evoked EPSCs from a CA1 pyramidal cell. (*B*) Example traces of electrically (upper) and optically (lower) evoked EPSCs. (*C*) Plot of normalized EPSC amplitude versus stimulus number.

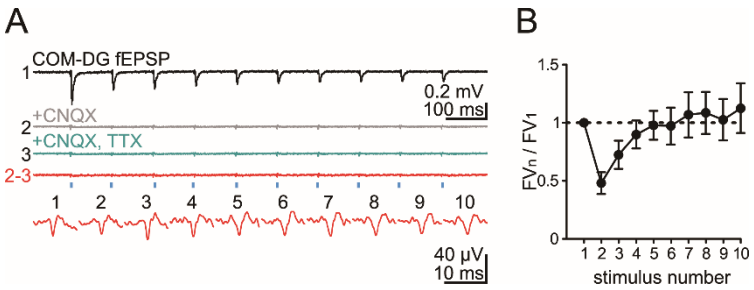

Figure S10. Recording of COM-evoked fiber volley

(*A*) Example traces of light-evoked field EPSPs (fEPSPs, black; trace 1), after addition of CNQX (10 µM, gray; trace 2) and after addition of CNQX (10 µM) and TTX (1 µM, cyan; trace 3), and subtracted trace (red; trace 2-3). Bottom trace, the TTX-sensitive fiber volleys (FVs), the enlargement of subtracted trace (red). (*B*) Plot of normalized FV versus stimulus number.

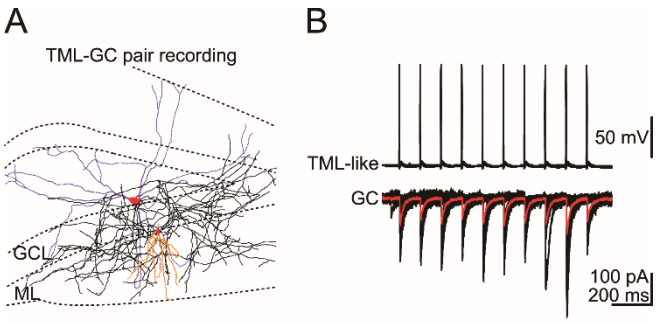

Figure S11. TML-like IN output to GCs

(*A*) An exemplar reconstruction of the recorded TML-like IN, in which dendrites, soma, and axons are shown in magenta, red, and black, respectively. The paired GC is shown, in which dendrites, soma, and axons are shown in orange, red and gray, respectively. (*B*) Paired recording from a TML-like IN-to-GC pair. Ten APs were evoked in the TML-like IN by injection of brief current pulses (2 ms, 10 Hz) every 20 s. Presynaptic INs were current clamped at –60 mV, whereas postsynaptic GCs were voltage clamped at –80 mV.

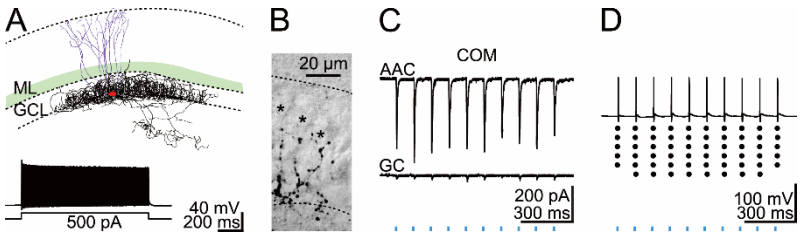

Figure S12. Reconstruction of an AAC-like cell

(*A*) Reconstruction of a biocytin-labeled AAC-like cell in the DG. The axon (black) of the labeled cell is mainly found in the GCL and the border between the GCL and hilus, where axon initial segments of GCs are localized. (*B*) High-power photomicrograph (an IR-DIC image and a single two-photon image are superimposed) shows axo-axonic cartridges (black) of the labeled AAC-like cell along the axon initial segment of three unstained GCs. Asterisks mark GC somata. (*C*) Upper, averaged traces from dual recording of an AAC-like cell and a GC; 10 Hz photo-stimulation of COM evoked EPSCs in the AAC-like cell and a GC. (*D*) Action potentials evoked in the AAC in response to 10 Hz photo-stimulation of COM. Spike raster plots below the traces show firing during six trials.